Noname manuscript No.
(will be inserted by the editor)

Local Binary Patterns for Image Quality Assessment: Performance Evaluation

Chi Hongyu, Quan Yuhui, Zhou Zihan, Mao Zhiming, Zhang Tianhao, Ding Yekai

Received: date / Accepted: date

Abstract Image quality assessment (IQA) aims at evaluating and quantizing the visual quality of images, which is very useful for various applications. In many scenarios, *e.g.* mobile applications, the computational recourse is limited, and thus the efficiency of IQA methods is critical. In this paper, we investigate a kind of reduced-reference IQA methods built upon local binary patterns (LBP), which is very efficient in computation and storage. Inspired by the fact that many variants of LBP that have been proposed are for different considerations, we first reviewed some representative LBP methods and then conducted a series of experiments to evaluate the performance of these LBP methods in IQA. Based on the experimental results, we compare the effectiveness of different LBP methods in IQA, as well as analyze the effect of LBP parameters on the performance. Such comparison and analysis provide very useful suggestions for IQA applications.

Keywords Image Quality Assessment · Performance evaluation · Local Binary Patterns

1 Introduction

With mobile devices becoming abundantly available, more and more visual data, such as images and videos, are generated and transmitted by mobile devices. In both the generation and the transition process, the visual quality of the mobile visual data is often degraded. Some often-seen degradation includes noises, blurring, ringing artifacts by lossy compression, etc. In computer science, the concept of image quality assessment (IQA) refers to quantizing the visual quality of images via computers[1], which is very useful for many applications. An example is, when mobile devices stream images to screens, the images are often compressed first to save bandwidth, and thus the streaming method needs an IQA method to estimate of visual quality of images and then balance the quality and compression rate.

Based on the degree of dependence on the reference image (i.e. the original image whose visual quality has no degradation), existing IQA methods can be divided into three categories: full-reference (FR) [3, 1], reduced-reference (RR) [4, 7] and no-reference (NR) [10, 8]. The FR method requires the whole reference image for assessment, while the NR approach directly quantifies the quality of given images without knowing the reference. In comparison with FR and NR approaches, the RR method requires only partial information from the reference image. Such partial information is often presented in some low-dimensional image quality features. The FR, RR, and NR methods have different applications. In this paper we focus on the RR method which is suitable for many mobile applications, considering the example of transmitting images, where only low-dimensional features of the reference images can be sent to the receivers for saving bandwidth. Moreover, an RR method can be easily combined with or developed to be an FR method, as the required information of an RR method is a subset of that of an FR method.

In many applications like mobile processing, the computational recourse is very limited. In such scenarios, the efficiency of an IQA method is a critical factor. This motivate us to investigate a kind of reduced-reference IQA methods built upon local binary patterns (LBP). The LBP-based methods are very suitable for mobile computing, as the LBP has advantages in fast computation. Moreover, the LBP are presented in the bit form which helps to save the mobile storage and facilitates the processing. Currently, there have been many LBP variants proposed with different considerations. Thus, there is a need to conduct a comprehensive per-

School of computer science and engineering, South China University of Technology, Guangzhou, China

[1] IQA via computers is also called objective IQA, while IQA via human is called subjective IQA.

formance evaluation on these LBP methods regarding IQA. Thus, in this paper, we first reviewed some representative LBP methods. Then, we conducted a series of experiments to evaluate the performance of these LBP methods in IQA. The experimental results include the effectiveness comparison of different LBP methods in IQA, as well as the analysis on the affect of LBP parameters to the performance. These comparison and analysis provide very useful suggestions for IQA applications.

1.1 Related Work

We first have a brief review on some recent RR-IQA methods, and then focus on some LBP-based IQA methods.

Many recent RR-IQA methods are based on natural image statistic models. In [4], Wang ,Simoncelli measure the K-L distance between the marginal probability distributions of wavelet coefficients. Li Q, Wang Z [5] compare statistical features extracted from divisive normalization transformation (DNT)-domain representations, using Gaussian scale mixture statistical model. In [6], Soundararajan and Bovik use the entropies of wavelet coefficients as measurement. Ma L, Li S, Zhang F, et al. [7] use generalized Gaussian density to model the discrete cosine transform (DCT) coefficient distributions.

In recent years, some methods based on LBP have been proposed. In [11], the LBP shifts between the reference and degraded images are utilized to describe structural degradation. In [12], Li Q et al. extract gradient-weighted histogram of LBP on the gradient map. Zhang M et al. [13] [14] use Laplacian of Gaussian filters to decompose the image into subband images and extract LBP or GLBP feature on these images.

1.2 Organization

This paper is organized as follows. In Section 2, we give a review on LBP and some of its variants. In Section 3, the experiment setup for performance evaluation is introduced. Then, the experimental results and analysis are presented in Section 4. Finally, Section 5 concludes the paper and discusses the future work.

2 Local Binary Patterns and Variants

2.1 Local Binary Pattern

The original local binary pattern (LBP) [15], proposed by Ojala et al., is a texture operator which characterizes the local image structure by coding the gray-value relationship between the center pixel and its 3×3 neighborhood. If the gray value of a neighborhood pixel is less than that of the center pixel, the neighborhood pixel is marked as 0, otherwise as 1. These labels are coded into a binary number with particular sequence. The corresponding decimal number is used as the center pixel's LBP value. See Figure 2 for an illustration. To adapt the operator to different scales, a circular symmetric neighborhood denoted by (P, R) is introduced, and the corresponding LBP operator is defined as follows:

$$LBP_{P,R} = \sum_{p=0}^{P-1} s(g_p - g_c)2^p \tag{1}$$

$$s(x) = \begin{cases} 1, & x \geq 0 \\ 0, & x < 0 \end{cases} \tag{2}$$

where P is the number of the sampled points in the neighborhood with radius R, g_p is the gray value of sampling point p and g_c is the gray value of the center pixel. Suppose the coordinate of g_c is $(0, 0)$, then the coordinate of g_p is given by $(R\cos(2\pi p/P), R\sin(2\pi p/P))$.

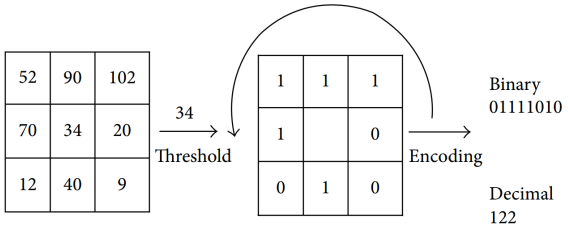

Fig. 1: Original LBP operator.

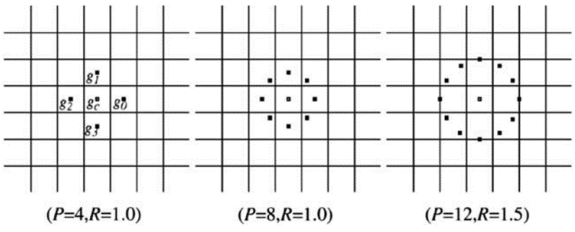

Fig. 2: $LBP_{P,R}$ operator Sampling points allocation.

Since the value if $LBP_{P,R}$ depends on the order of 1s and 0s, e.g. 1100 and 0110 corresponding to the same pattern but different decimal value, the LBP operator is sensitive to rotation. A rotation-invariant LBP operator was proposed by Ojala et al. [16] as follows:

$$LBP^{ri}_{P,R} = min\{ROR(LBP_{P,R}, i)|i = 0, 1, ..., P-1\} \tag{3}$$

where $ROR(x, i)$ performs a circular bit-wise right shift on the P-bit number x i times. By using ROR, the LBP binary code is transformed into its minimum value, and then the rotation invariance is achieved. For example, after the ROR operation, 1100 and 0110 are transformed into a same minimum value 3.

However, even with rotation-invariance, the pattern number of LBP is very large, e.g. the $LBP^{ri}_{8,R}$ operator has 36 individual patterns. Ojala et at. observed that certain local binary patterns are fundamental properties of texture. To define these patterns, a uniformity measure U, which corresponds to the number of bite wise 0/1 changes [17], is introduced as follows:

$$U(LBP_{P,R}) = |s(g_{p-1} - g_c) - s(g_0 - g_c)| + \sum_{p=1}^{P-1} |s(g_p - g_c) - s(g_{p-1} - g_c))|. \quad (4)$$

and the corresponding uniform rotation-invariant LBP operator is defined as:

$$LBP^{riu2}_{P,R} = \begin{cases} LBP^{ri}_{P,R}, \text{ if } U(LBP_{P,R} \leq 2) ; \\ P + 1, \quad \text{otherwise.} \end{cases} \quad (5)$$

As all the non-uniform patterns are assigned to the same value, the length of LBP-based features are reduced. Moreover, as the pattern with frequent bit-wise changes often correspond to noise patterns, the operator's robustness of noise is improved.

2.2 Local Ternary Pattern

The above LBP operators only consider the sign of different between the center pixel and neighbors, which discards magnitude information. To utilize the magnitude information for improving the discriminative of LBP. Tan et al. extended LBP to 3-value code by giving an threshold t [18]. The LTP operator can be written as follows:

$$LTP_{P,R} = \sum_{p=0}^{P-1} 2^p s(g_p - gc), \quad s(x) = \begin{cases} 1, & x \geq t \\ 0, & -t < x < t \\ -1, & x \leq -t \end{cases} \quad (6)$$

Then the LTP operator is separated into upper pattern and lower pattern, see Figure 3 for an illustration. As utilizing magnitude information, the LTP is more discriminative compared to LBP. Moreover, it is shown that the robustness of LTP to noise is better than LBP [18].

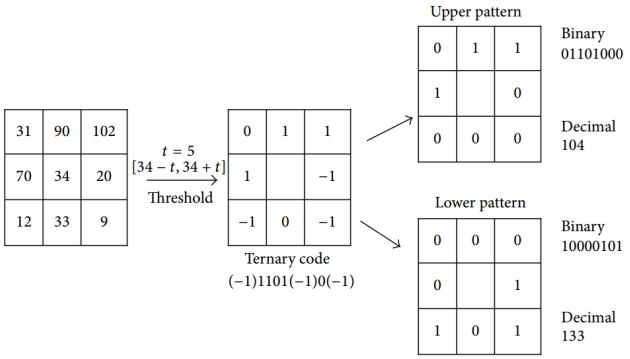

Fig. 3: LTP operator.

2.3 Completed Local Binary Pattern

The above LBP operators only encode the magnitude orders of pixels, while the magnitude difference between the center pixel and the neighborhood is not considered. Moreover, the value of the center pixel, which may be useful, is discard. To utilize these information, the completed local binary pattern (CLBP) [19] characterizes the information of magnitude and the center pixel by binary codes individually. The CLBP is composed of three parts: the sign (CLBP_S), the magnitude (CLBP_M) and the center gray level (CLBP_C). The CLBP_S is equivalent to the traditional LBP defined in Eq. (1). The coding strategy of CLBP_M and CLBP_C is similar to that of the LBP, which is defined as:

$$CLBP\_M_{P,R} = \sum_{p=0}^{P-1} s(m_p - c), \quad (7)$$

$$CLBP\_C_{P,R} = s(g_c - I) \quad (8)$$

where s is the thresholding function defined in Eq. (2), m_p is the magnitude of sampling point p and the center pixel, c is the mean value of m_p in the whole image, g_c is the gray value of center pixel and I is the average gray level of the whole image. By combining these three features, significant improvement can be achieved.

2.4 Complete Local Ternary Pattern

As LTP has characteristic of combining with other operators, Taha et al. proposed a completed modeling of the local ternary pattern operator [20], which combines the LTP and the CLBP, to enhance the discriminating property. Each part has two complementary components (upper and lower). The

representation of sign information can be written as follows:

$$CLTP\_S^{upper}_{P,R} = \sum_{p=0}^{P-1} 2^p s^{upper}(g_p - (g_c + t)),$$
$$s_p^{upper}(x) = \begin{cases} 1, & x \geq 0 \\ 0, & \text{otherwise} \end{cases} \tag{9}$$

$$CLTP\_S^{lower}_{P,R} = \sum_{p=0}^{P-1} 2^p s^{lower}(g_p - (g_c - t)),$$
$$s_p^{lower}(x) = \begin{cases} 1, & x < 0 \\ 0, & \text{otherwise} \end{cases} \tag{10}$$

where the P, R, g_p and g_c are defined in Eq. (1), t is the user-defined threshold. Similar to $CLTP\_S^{upper}_{P,R}$ and $CLTP\_S^{lower}_{P,R}$, the magnitude part can be written as follows:

$$CLTP\_M^{upper}_{P,R} = \sum_{p=0}^{P-1} 2^p s^{upper}(|g_p - g_c| - (c + t)), \tag{11}$$

$$CLTP\_S^{lower}_{P,R} = \sum_{p=0}^{P-1} 2^p s^{lower}(|g_p - g_c| - (c - t)), \tag{12}$$

Moreover, $CLTP\_C^{upper}_{P,R}$ and $CLTP\_C^{lower}_{P,R}$ can be described as follows:

$$CLTP\_C^{upper}_{P,R} = s^{upper}(g_c - (I + t)), \tag{13}$$

$$CLTP\_C^{lower}_{P,R} = s^{lower}(g_c - (I - t)), \tag{14}$$

where the I is defined in Eq. (8). The threshold t can be different in three component parts.

2.5 Local Binary Pattern Variant

The way that LBPV utilizes magnitude information differs from these methods mentioned above. LBPV use the variance of neighborhood as the center pixel's weight in histogram calculation. The principle is that the high frequency region tends to have a large variance and a large contribution to the texture. The variance of the center point's neighborhood is defined as follows:

$$VAR_{P,R} = \frac{1}{p} \sum_{p=0}^{P-1} (g_p - u)^2 \tag{15}$$

$$u = \frac{1}{p} \sum_{p=0}^{P-1} g_p \tag{16}$$

The variance is taken as the weight of histogram. The resulting histogram vector is the LBPV feature, defined as follows:

$$LBPV_{P,R}(k) = \sum_{i=1}^{N} \sum_{j=1}^{M} w(LBP_{P,R}(i,j), k), \quad k \in [0, K] \tag{17}$$

$$w(LBP_{P,R}(i,j), k) = \begin{cases} VAR_{P,R}(i,j), & LBP_{P,R}(i,j) = k \\ 0, & \text{otherwise} \end{cases} \tag{18}$$

where K is the number of LBP patterns. LBPV traverses each LBP value for weighted histogram statistics. In general image applications, extracting LBPV features from a whole image will lose texture's spatial information. So the LBPV feature is extracted from each block after dividing the image.

3 Experimental Setup

3.1 Outline

In this section, we will introduce the outline of the experiment and some details. The outline is illustrated in Fig. 4. Preprocessing is performed first. The image is transformed into gray-scale with uniform size. The LBP feature is extracted from the reference image and the degraded image respectively. The difference of features between reference and degraded images is objective score. By a non-linear function, objective score is mapped to subjective score.

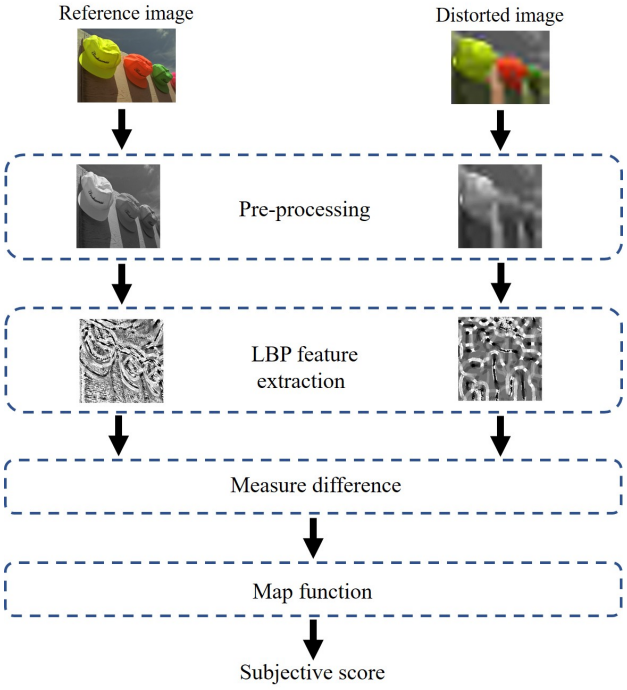

Fig. 4: Outline of proposed method.

After preprocessing, the LBP features are extracted from the image. The principle of using LBP is that when the image is degraded, such as having noise, the texture around

noise will change, as well as it's LBP value. The degree of degradation can be assessed by measuring the change of the LBP value.

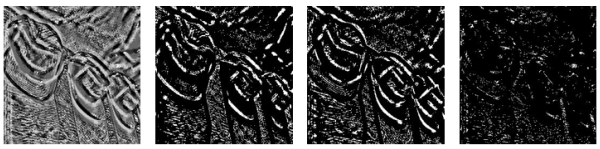

Fig. 5: $LBP^{riu2}_{P,R}$ code maps. From left to right, the first is the LBP feature image of a reference image. The second to last are the code maps when LBP value equal to 0,4,5.

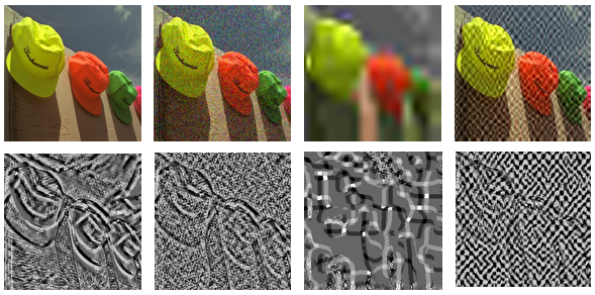

Fig. 6: $LBP^{riu2}_{P,R}$ code for some degraded images. The first row correspond to a reference image and three degraded images. The second row are their corresponding LBP feature images.

The common statistical methods of distance are L0, L1 or L2. Each of them can measures difference of features. In our implementation, we use L0 norm. One LBP value represents one specific texture feature. The difference between texture features is hard to be quantized with distance. For example, the L1 norm of difference between 00000001 and 00010001 is 32, but that between 0000-0011 and 00000011 is 2. The scale can not represent the relationship between features. On the country, it may interference image degradation assessment.

As objective scores and the subjective ranting have a nonlinear relationship [21], a function f [22]is utilized to map the estimated objective score x to the subjective score $f(x)$, which is defined as:

$$f(x) = \beta_1(\frac{1}{2} - \frac{1}{1 + exp(\beta_2(x - \beta_3))}) + \beta_4 x + \beta_5 \quad (19)$$

where β_1,β_2,...,β_5 are determined by least squares fitting between the mapped objective scores and the subjective rating.

Table 1: Major Characteristics of Databases

Database	Reference img	Distorted img	Dist. Types
TID2008	25	1700	17
CSIQ	30	866	6
LIVE	29	779	5
IVC	10	185	4
MICT	14	168	2
WIQ	7	80	1
A57	3	54	6

3.2 Benchmark Databases and Evaluation Criterion

The experiment is based on seven public benchmark database: the A57 database [23],the WIQ database [24], the MICT database [25], the IVC databasethe [26], the LIVE database [27], the CSIQ database [28], and the TID2008 database [29]. The major characteristics of these databases, including the number of reference images, the number of distorted images and the number of distortion types, are listed in Table 1.

Five widely-used measures are chosen to evaluate performance. Two measure the monotonicity: the Spearman rank-order correlation coefficient (SROCC) and the Kendall rank-order correlation coefficient (KROCC). There measure the prediction accuracy: The Pearson linear correlation coefficient (PLCC), the Root mean square error (RMSE) and the Mean absolute error (MAE). For a desirable RR-IQA method, the value of SROCC, KROCC and PLCC are expected to be high, while that of RMSE and MAE are expected to be low.

Not all of these methods were implemented. We only refer the result that are available.

The test was perform on AMD AF-8150 processor and 32GB RAM. The software platform is Matlab R2016a on Windows 10.

4 Experimental Results

In this section, we show performance of LBP based methods on seven benchmark database and give a brief analysis of the experimental results

4.1 Arguments Change

Before the feature extraction, the image is normalized firstly. In Table 3, we compare the performance of different normalized size on LIVE database.

There are three kinds of LBP features extracted from an image: LBP feature histogram, LBP feature graph, and histogram of each block after dividing LBP feature graph, which are marked as LBP_hist, LBP_img, LBP_block_hist.

The extraction of LBP features involves three parameters: the radius of LBP operator, the number of sampling,

Table 2: The Performance by LBP_img Versus Image Size on the LIVE Database

	512×512	256×256	128 ×128
PLCC	0.9248	0.8672	0.8925
SROOC	0.9185	0.9200	0.8925
KROOC	0.7508	0.7502	0.7185
RMSE	10.3955	13.6038	12.3235
MAE	8.2168	10.9424	9.9936

Table 3: The Performance of different feature types on the LIVE, CSIQ, TID2008 Database

		LBP_hist	LBP_block_hist	LBP_img
LIVE	PLCC	0.7355	0.8672	0.7947
	SROOC	0.7617	0.9200	0.8803
	KROOC	0.5652	0.7502	0.6949
	RMSE	18.5111	13.6038	16.5859
	MAE	14.4359	10.9424	13.3539
CSIQ	PLCC	0.7135	0.6388	0.7783
	SROOC	0.6307	0.7751	0.7409
	KROOC	0.4588	0.5960	0.5568
	RMSE	0.1840	0.2020	0.1649
	MAE	0.1505	0.1713	0.1319
TID2008	PLCC	0.5346	0.3842	0.6971
	SROOC	0.4310	0.5879	0.6711
	KROOC	0.3025	0.4338	0.4883
	RMSE	1.1341	1.2389	0.9622
	MAE	0.9443	0.9992	0.7559

and the size of block when LBP_block_hist is used. In Figure 7, we summarize the SROOC result of LBP_img under different parameters.

The length of the radius represents the scale of the texture described. For example, for a large wavy texture, the LBP operator with a small radius can not cover the shape of the entire wave, but only a small part. Then the value calculated by LBP may represent a semicircular arc. This makes it very crucial for a fixed radius of the LBP operator to find a scale suitable for the image .

The number of samples represents how many points are compared with the center point. It is not advisable to increase performance by increasing the number of neighborhood. As can be seen from the experimental results, for the 12 sampling points and 16 sampling points, the performance declines. When the sampling points increase, a pixel is neighbors for more center points. A small noise influence more neighbors' LBP values. So the degree of degradation becomes hard to be distinguished.

To reduce the feature length, LBP_block_hist divides the image into multiple blocks and then counts the histogram of the LBP value on each block. If the LBP diagram is used as a feature, the spatial information of the texture can be retained extremely. But Its shortcoming is obvious. The length of the

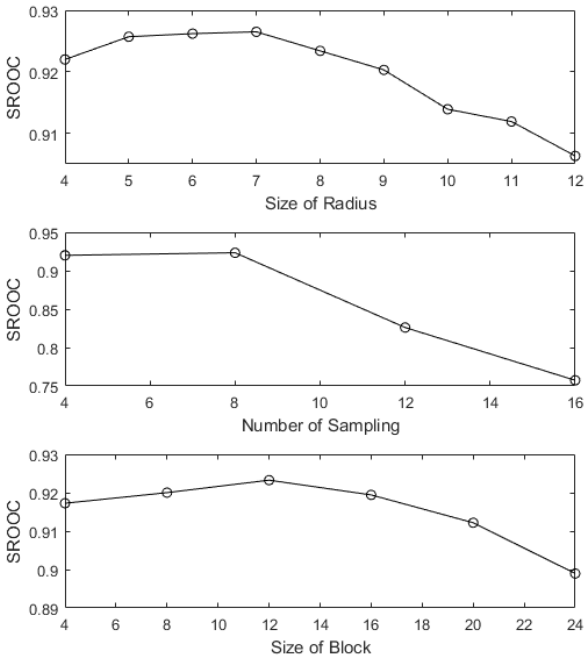

Fig. 7: The performance of LBP_img in terms of SROOC vs. size of radius/number of sampling/size of block on the LIVE database.

feature is not reduced. So there is a trade-off between feature length and effect. The results shows that with the block being bigger and bigger, the spatial information is lost and the effect is decreased gradually.

Considering the feature length and performance, the parameters of LBP operator in our experiment are set as follows:

- the normalized size: 256×256
- the size of radius: 8
- the number of sampling: 4
- the size of block: 12×12

4.2 Performance

The performance of the proposed approaches and the compared approaches are listed in Table 4. The method which performs the best on each criteria is marked in boldface. The method which performs the best in LBP-based methods is marked in underline.

M-LBP is the multi-scale LBP. The LBP operators with different radius are used to extract the features of an image. Then these features are aggregated as the final total feature. M-LBP is more effective than LBP_img on most of database. The performance of LTP is comparable to LBP_img in seven databases. CLBP and CLTP perform best in LBP-based methods. CLTP is a little better than CLBP on TID2008

Table 4: Performance Comparison on Seven Benchmark Database

Database	Criteria	Reduced Reference									
		LBP_img	M-LBP	LTP	CLBP	CLTP	LBPV	RR-SSIM [30]	HWD2 [31]	WNISM [2]	RRED [6]
A57	PLCC	0.8890	0.7170	0.8776	0.8752	**0.9436**	0.7215	0.7044	N/A	0.5125	0.8547
	SROOC	0.8407	0.7361	0.8120	0.8747	**0.9236**	0.6870	0.7301	N/A	0.3140	0.8399
	KROOC	0.6706	0.5420	0.6399	0.6958	**0.7797**	0.5392	0.5345	N/A	0.2210	0.6483
	RMSE	0.1126	0.1713	0.1178	0.1189	**0.0814**	0.1702	0.1744	N/A	0.2317	0.1276
	MAE	0.0881	0.1445	0.0899	0.0993	**0.0689**	0.1365	0.1433	N/A	0.1971	0.1051
WIQ	PLCC	0.6224	0.7106	0.5830	0.6879	0.6634	0.6833	N/A	N/A	0.3401	**0.8367**
	SROOC	0.6458	0.6882	0.6407	0.6992	0.6820	0.7592	N/A	N/A	0.2156	**0.7626**
	KROOC	0.4961	0.5132	0.4940	0.5271	0.5227	0.5613	N/A	N/A	0.1561	**0.5864**
	RMSE	17.9280	16.1175	18.6109	16.6259	17.1404	16.7238	N/A	N/A	21.5404	**12.5448**
	MAE	14.9408	13.1387	15.4986	13.9470	14.2265	13.0803	N/A	N/A	16.9682	**9.8095**
MICT	PLCC	0.5715	0.7933	0.5445	**0.8603**	0.7685	0.4085	0.8051	N/A	0.6542	0.8272
	SROOC	0.5968	0.7980	0.5717	**0.8736**	0.8034	0.4552	0.8003	N/A	0.6322	0.8228
	KROOC	0.4229	0.6164	0.4047	**0.6893**	0.6106	0.3220	0.6090	N/A	0.4570	0.6306
	RMSE	1.0270	0.7619	1.0498	**0.6380**	0.8008	1.1424	0.7423	N/A	0.9464	0.7033
	MAE	0.8798	0.5921	0.9061	**0.4965**	0.6673	1.0062	0.5648	N/A	0.7742	0.5465
IVC	PLCC	0.6798	0.8407	0.6545	0.8303	0.7161	0.7657	0.8177	N/A	0.5311	**0.9050**
	SROOC	0.7486	0.8547	0.7458	0.8646	0.7880	0.7801	0.8154	N/A	0.4114	**0.8987**
	KROOC	0.5755	0.6565	0.5781	0.6803	0.6159	0.5786	0.6164	N/A	0.2907	**0.7175**
	RMSE	0.8935	0.6597	0.9212	0.6790	0.8504	0.7836	0.7014	N/A	1.0322	**0.5183**
	MAE	0.7429	0.5368	0.7726	0.5471	0.6948	0.6339	0.5619	N/A	0.8550	**0.3971**
LIVE	PLCC	0.7947	0.9240	0.7553	0.9300	0.8798	0.6788	0.9194	**0.9624**	0.7365	0.9385
	SROOC	0.8803	0.9181	0.8645	**0.9495**	0.9395	0.7288	0.9129	0.9418	0.7472	0.9429
	KROOC	0.6949	0.7495	0.6746	**0.8026**	0.7844	0.5381	0.7349	N/A	0.5577	0.7888
	RMSE	16.5859	10.4493	17.9065	10.0428	12.9892	20.0629	11.3026	**6.3657**	18.4814	**9.4317**
	MAE	13.3539	8.3027	14.5436	8.0407	10.3462	16.6017	9.1889	**4.8445**	14.6352	**7.2976**
CSIQ	PLCC	0.7783	0.8152	0.7569	0.8702	0.8612	0.5571	0.8426	N/A	0.7124	**0.9121**
	SROOC	0.7409	0.7781	0.7276	0.8150	0.8033	0.7311	0.8527	N/A	0.7431	**0.9184**
	KROOC	0.5568	0.5934	0.5402	0.6512	0.6405	0.5283	0.6540	N/A	0.5457	**0.7429**
	RMSE	0.1649	0.1520	0.1716	0.1293	0.1334	0.2180	0.1413	N/A	0.1842	**0.1077**
	MAE	0.1319	0.1186	0.1384	0.0980	0.1038	0.1784	0.1092	N/A	0.1492	**0.0820**
TID2008	PLCC	0.6971	0.6352	0.6890	0.7318	0.7668	0.4183	0.7231	N/A	0.5891	**0.8255**
	SROOC	0.6711	0.6143	0.6722	0.6898	0.7283	0.5262	0.7231	N/A	0.5119	**0.8237**
	KROOC	0.4883	0.4507	0.4876	0.5167	0.5434	0.3780	0.7231	N/A	0.3589	**0.6346**
	RMSE	0.9622	1.0364	0.9726	0.9146	0.8613	1.2189	0.7231	N/A	1.0843	**0.7573**
	MAE	0.7559	0.8190	0.7695	0.7219	0.6758	0.9669	0.7231	N/A	0.8666	**0.5641**

Table 5: Avrage Time Cost of An Image on the LIVE Databse

method	LBP_img	M-LBP	LTP	CLBP	CLTP	LBPV	RR-SSIM [30]	HWD2 [31]	WNISM [2]	RRED [6]
time	0.11	0.32	0.10	0.11	0.14	0.15	2.74	N/A	N/A	6.49

database. LBPV performs good on the small and medium-sized database. But on large databases such as CSIQ and TID2008, LBPV is a little poor. It can be seen that the more descriptive the descriptor is, the more accurate assessment will be achieved.

Compared with other mainstream methods,the average performance of LBP-based methods is comparable to that of SSIM and is better than that of WNISM. But compared with RRED, there are some deficiencies, especially on the ITD2008 database which is large and complex.

In general, each LBP-based image quality assessment algorithm listed in this paper has capability to evaluate the degradation of images. CLBP and CLTP are more suitable for complex and realistic scenes.

The experiment records the time (in seconds) taken by each algorithm. The results are listed in Table 5. From the table it can be concluded that the time of LBP-based methods is much smaller than compared methods. In LBP-based methods, M-LBP is the longest time consuming because it needs to count multiple LBP features. Even then it is 1/9 of SSIM time-consuming, 1/20 of RRED time-consuming. Therefore, the LBP-based methods have advantages in efficiency.

5 Conclusion

Image quality assessment is an important research direction in image processing. However, the previous method is not suitable for mobile devices and real-time evaluation in terms of computation cost and hardware requirements. LBP feature extraction process is simple and fast, with low requirement of hardware. We evaluated the performance of some RR-IQA algorithms based on LBP and test the different parameters: radius, the number of sampling points, block size.

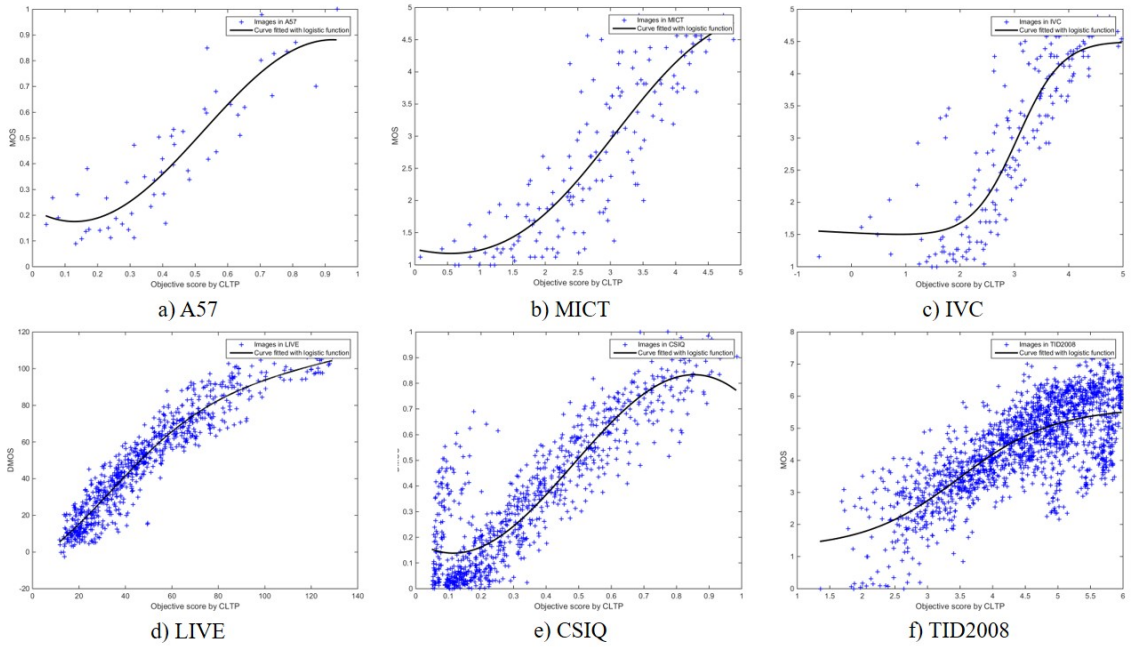

Fig. 8: Scatter plots of the predicted scores against the subvjective scores by CLTP on six databases.

By analyzing the experimental results, the recommended parameter settings are given. We tested the performance of these methods on seven widely used databases and analyzed the results. The LBP image is used as features to preserve the spatial information of the texture, which helps to detect the degradation in the image. CLBP and CLTP show good results on seven databases, especially the TID2008 database. From the time point of view, the methods meet the characteristics of fast. The time spent is far less than compared methods. However, the performance of LBP-based methods have yet to be improved. In the future, we will try to improve performance by proposing new LBP variants.

References

1. Zhang L, Zhang D, Mou X, et al. FSIM: A Feature Similarity Index for Image Quality Assessment[J]. Image Processing IEEE Transactions on, 2011, 20(8):2378-2386.
2. Wang Z, Wu G, Sheikh H R, et al. Quality-aware images[J]. IEEE Transactions on Image Processing, 2006, 15(6):1680-1689.
3. Wang Z, Bovik A C, Sheikh H R, et al. Image quality assessment: from error visibility to structural similarity[J]. IEEE Transactions on Image Processing, 2004, 13(4):600-612.
4. Wang Z, Simoncelli E P. Reduced-reference image quality assessment using a wavelet-domain natural image statistic model[C]// Electronic Imaging. International Society for Optics and Photonics, 2005:149–159.
5. Li Q, Wang Z. Reduced-Reference Image Quality Assessment Using Divisive Normalization-Based Image Representation[J]. IEEE Journal of Selected Topics in Signal Processing, 2009, 3(2):202-211.
6. Soundararajan R, Bovik A C. RRED Indices: Reduced Reference Entropic Differencing for Image Quality Assessment[J]. IEEE Transactions on Image Processing A Publication of the IEEE Signal Processing Society, 2011, 21(2):517-526.
7. Ma L, Li S, Zhang F, et al. Reduced-Reference Image Quality Assessment Using Reorganized DCT-Based Image Representation[J]. IEEE Transactions on Multimedia, 2011, 13(4):824-829.
8. Sheikh H R, Bovik A C, Cormack L. No-reference quality assessment using natural scene statistics: JPEG2000[J]. IEEE Transactions on Image Processing, 2005, 14(11):1918-1927.
9. Wang Z, Bovik A C, Evan B L. Blind measurement of blocking artifacts in images[C]// International Conference on Image Processing, 2000. Proceedings. IEEE, 2000:981-984 vol.3.
10. Wang Z, Sheikh H R, Bovik A C. No-reference perceptual quality assessment of JPEG compressed images[C]// International Conference on Image Processing. 2002. Proceedings. IEEE, 2002:I-477-I-480 vol.1.
11. Wu J, Lin W, Shi G. Image Quality Assessment with Degradation on Spatial Structure[J]. IEEE Signal Processing Letters, 2014, 21(4):437-440.
12. Li Q, Lin W, Fang Y. No-Reference Quality Assessment for Multiply-Distorted Images in Gradient Domain[J]. IEEE Signal Processing Letters, 2016, 23(4):1-1.
13. Zhang M, Xie J, Zhou X, et al. No reference image quality assessment based on local binary pattern statistics[C]// Visual Communications and Image Processing. 2013:1-6.
14. Zhang M, Muramatsu C, Zhou X, et al. Blind Image Quality Assessment Using the Joint Statistics of Generalized Local Binary Pattern[J]. IEEE Signal Processing Letters, 2015, 22(2):207-210.
15. Ojala T, Harwood I. A Comparative Study of Texture Measures with Classification Based on Feature Distributions[J]. Pattern Recognition, 1996, 29(1):51-59.
16. Ojala T, Pietik, Inen M, et al. Gray Scale and Rotation Invariant Texture Classification with Local Binary Patterns[C]// European Conference on Computer Vision. Springer-Verlag, 2000:404-420.
17. Ojala T, Pietik, Inen M, et al. Multiresolution Gray-Scale and Rotation Invariant Texture Classification with Local Binary Patterns[J]. Pattern Analysis & Machine Intelligence IEEE Transactions on, 2002, 24(7):971-987.

18. Tan X, Triggs B. Enhanced Local Texture Feature Sets for Face Recognition Under Difficult Lighting Conditions[J]. IEEE Transactions on Image Processing A Publication of the IEEE Signal Processing Society, 2010, 19(6):1635-1650.
19. Guo Z, Zhang L, Zhang D. A completed modeling of local binary pattern operator for texture classification.[J]. IEEE Transactions on Image Processing A Publication of the IEEE Signal Processing Society, 2010, 19(6):1657-1663.
20. Rassem T H, Khoo B E. Completed Local Ternary Pattern for Rotation Invariant Texture Classification[J]. Scientific World Journal, 2014, 2014(1):10.
21. Antkowiak J, Baina T J. FINAL REPORT FROM THE VIDEO QUALITY EXPERTS GROUP ON THE VALIDATION OF OBJECTIVE MODELS OF VIDEO QUALITY ASSESSMENT March[J]. ITU-T Standards Contribution COM, 2000.
22. Sheikh H R, Sabir M F, Bovik A C. A statistical evaluation of recent full reference image quality assessment algorithms.[J]. IEEE Transactions on Image Processing, 2006, 15(11):3440-3451.
23. Chandler D M, Hemami S S. A57 database[J]. 2012-10-7]. http://foulard. ece. coruell, edu/dmc27/vsnr/vsnr, ht-ml, 2007.
24. Engelke U, Zepernick H J, Kusuma M. Wireless imaging quality database[J]. h ttp://www. bth. se/tek/rcg. nsf/pages/wiq-db, 2010.
25. Horita Y, Shibata K, Kawayoke Y, et al. MICT image quality evaluation database[J]. Online], http://mict. eng. u-toyama. ac. jp/mictdb. html, 2011.
26. Ninassi A, Le Callet P, Autrusseau F. Subjective quality assessment-IVC database[J]. Online], http://www2. irccyn. ec-nanates. fr/ivcdb, 2006.
27. Sheikh H R, Wang Z, Bovik A C, et al. Image and video quality assessment research at LIVE[J]. 2003.
28. Larson E C, Chandler D M. Categorical subjective image quality CSIQ database[J]. 2009.
29. Ponomarenko N, Lukin V, Zelensky A, et al. TID2008-a database for evaluation of full-reference visual quality assessment metrics[J]. Advances of Modern Radioelectronics, 2009, 10(4): 30-45.
30. Rehman, Wang. Reduced-reference image quality assessment by structural similarity estimation.[J]. IEEE Transactions on Image Processing, 2012, 21(8):3378-89.
31. Gao X, Lu W, Tao D, et al. Image quality assessment based on multiscale geometric analysis[J]. IEEE Transactions on Image Processing A Publication of the IEEE Signal Processing Society, 2009, 18(7):1409-23.